

Improved Torque and Speed Performances for DTC Controlled Asynchronous Machine By Fuzzy Switching Algorithm

Goksu Gorel*, Wahib Hilouan Mohamed

Çankırı Karatekin University, Faculty of Engineering, Department of Electronic and Electrical, Çankırı, Türkiye

*goksugorel@karatekin.edu.tr^{ID}, wahibhilouan@gmail.com^{ID}

Received date:27.05.2022, Accepted date: 29.12.2022

Abstract

Direct Torque Control (DTC) is a vector control method based on the control of the stator flux vector in the desired direction. The control of the stator flux vector is achieved by direct selection of the optimum inverter output voltage vectors. The limit values of the trajectory determined in the rotation of the stator flux vector are determined using hysteresis controllers. In this study, performance analysis of two different control methods for reducing speed and torque oscillations of a three-phase asynchronous motor controlled by direct torque control are presented. In Matlab/Simulink based simulation studies, performance analyses were made for different speed and torque references of the motor, and both the transient and steady state speed and torque changes were presented comparatively. When the obtained results are examined, it is seen that the performance of the new fuzzy-based controller, which is offered instead of the Proportional Integral Derivative (PID) controller used in traditional control, significantly decreases in the specific conditions of motor speed and torque oscillations. However, considering the control structure of the direct torque controller, the simple and plain control structure has been preserved. According to the results obtained, it has been shown that the Fuzzy Logic (FL) controller gives a better result than the PID controller at $t=4.5$ seconds.

Keywords: Asynchronous machine, DTC, FL, PID controller

Bulanık Anahtarlama Algoritması ile DTC Kontrollü Asenkron Makine için İyileştirilmiş Tork ve Hız Performansları

Öz

Doğrudan moment kontrolü, stator akı vektörünün istenilen yörüngede kontrolü esasına dayalı bir vektör kontrol yöntemidir. Stator akı vektörünün kontrolü, optimum evirici çıkış gerilim vektörlerinin doğrudan seçimi ile sağlanmaktadır. Stator akı vektörünün dönüşünde belirlenen yörüngenin sınır değerleri, histerezis denetleyicilerin kullanımı ile belirlenir. Bu çalışmada, doğrudan moment denetimi ile denetlenen üç fazlı bir asenkron motorun, hız ve moment salınımlarının azaltılmasına yönelik iki farklı kontrol yönteminin performans analizleri sunulmuştur. Matlab/Simulink tabanlı benzetim çalışmalarında motorun farklı hız ve moment referansları için performans analizleri yapılmış gerek geçici durum ve gerekse kararlı durum hız ve moment değişimleri karşılaştırmalı olarak sunulmuştur. Elde edilen sonuçlar incelendiğinde, geleneksel denetimde kullanılan PID kontrolörü yerine sunulan yeni bulanık tabanlı denetleyici performansının motor hız ve moment salınımlarının spesifik şartlarında belirgin ölçüde azalma sağlandığı görülmüştür. Bununla birlikte, doğrudan moment denetleyicinin denetim yapısı dikkate alındığında, basit ve sade denetim yapısı korunmuştur. Elde edilen sonuçlara göre FL kontrolörün PID kontrolöründen daha iyi bir sonuç verdiği $t=4.5$ saniyesinde gösterilmiştir.

Anahtar Kelimeler: Asenkron motoru, DTC, FL, PID kontrolör

INTRODUCTION

The asynchronous machine, due to its low cost and robustness, is currently the most widely used machine for achieving speed variations. The asynchronous machine has a default unlike the DC machine. That means that the power supply causes the same current to create the flux and the torque, by

causing a flux variation obtained by the torque variations, which makes the control still much more complex than usual. However, numerous studies have been carried out to ensure that the machine is controlled by using of electronic power systems, offering performance and dynamism.

Direct torque control, around the 1980s a so-called Takashi implemented a method that focuses on the torque and flux of the machine. The DTC is the quickest, simplest, and most precise torque control approach for IM drives. It is well recognised for being resilient to changes in motor characteristics, with the exception of stator resistance. Even though it is simple and provides significant benefits, the biggest disadvantage was the wide band of the inverter's switching frequency, even when the flux and torque references were kept constant. This is owing to the nature of the torque and flux hysteresis controllers utilised. The introduction of constant sampling techniques, which replace traditional analogue hysteresis controllers, was the second phase in the development of the DTC concept. As a result, the inverter's maximum switching frequency is restricted. Several writers have proposed numerous modifications and variations to the DTC concept in the case of constant sample frequency. The most of them, however, do not give the quickest torque response (El-Shimy and Zaid, 2016).

The purpose of this method is to estimate the torque and flux of the machine, which is supplied by a two-stage voltage inverter. At high speeds, the method is not sensitive to machine's parameters. This is not the case in low speed, where stator resistance plays an important role in flux estimation. In past decades researchers tried to come up with kindly solutions to provide a good performance to DTC (Soukaina E. D. et al. 2022). Consequently, regulators such as artificial intelligence as fuzzy logic and PID regulator will be used for the rest of our article in order to reduce torque ripple. One of the most important aspects of an IM drive is speed control, which must be managed effectively in order to achieve optimum results. For decades, the proportional integral controller seems to be the choice for induction motor drive's speed control because of its simple structure and capacity to make a fast response time with optimizing parameters. However, because of the PI's nature with fixed gains, if the parameters, speed, or load are modified, the drive performance may deteriorate. As a result, a very durable controller is required, one which can react to changes towards the motor drive. The fuzzy logic controller (FLC) has been recommended as an advanced speed controller due to its capacity to deal with systems non-linearities, measurement variations, and speed variances (Farah *et al.* 2021).

DIRECT TORQUE CONTROL OF INDUCTION MACHINE

The Direct Torque Control (DTC) technique was introduced by Takahashi in the mid-1980s. Recently, it has been increasingly used in the industry in place of other types, especially Field Oriented Control (FOC). Several works have enabled a rigorous modeling of this control technique, which examines the potential of implementing a torque and flux to AC machines in a decoupled manner when fed by a voltage converter without the need of a feedback loop for current regulation, achieving performance comparable to vector controls. Without the need of electromechanical sensors, the DTC calculates the controlling quantities of stator flux and torque of the motor using stator current measurements (Perdukova et al 2020). In the DTC structure, the asynchronous machine controlled by the voltage inverter is a hybrid dynamic system, whose continuous part is the asynchronous machine and whose discrete part is the voltage inverter (Said M. et al. 2022).

Many different control systems for induction motors have been developed in recent years, and direct torque control has risen to relevance due to its fast dynamic torque feedback and simple control structures. However, the direct torque control approach still has several disadvantages over other control systems, the most significant of which is excessive torque ripple (Korkmaz *et al.* 2015).

The control consists of determining the control sequence supplied to the switching of a voltage inverter in terms of controlling the electromagnetic torque and stator flux. This choice is designed to take advantage of hysteresis controllers, which are responsible for controlling the system's state while taking into account the stator flux amplitude and electromagnetic torque (Mustapha *et al.* 2022). To keep these two quantities within defined error ranges. The two outputs of the controllers combined with the information on the position where the flux vector was located, determine the switching table used to regulate the inverter. The inverter (two-level inverter) can reach seven different positions in the phase plane, corresponding to the eight sequences of the voltage vector at the inverter output. The direct control of the conventional torque of a three-phase asynchronous machine can be illustrated in Figure 1.

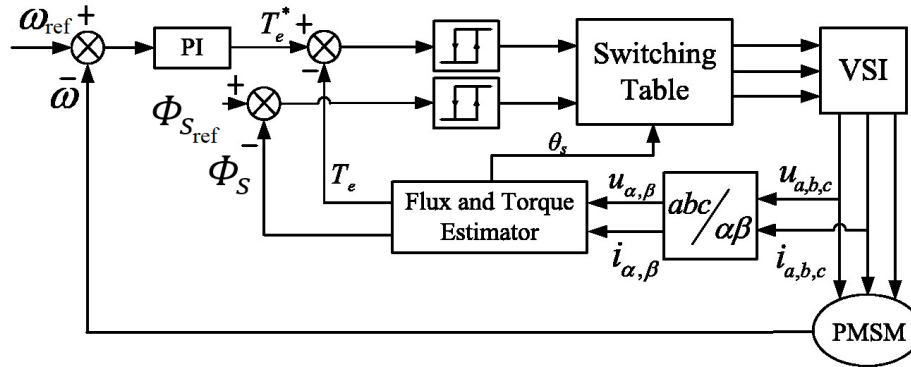


Figure 1. Structure of conventional direct torque control

Mathematical Modeling of IM and Voltage Source Inverter

The simplified equation 1 of the model of the induction machine in the stator reference (α, β) in steady state is shown below:

$$\dot{x} = Ax + B \tag{1}$$

With, $A = \begin{bmatrix} a_1 & 0 & a_2 & a_{3\omega_r} \\ 0 & a_1 & -a_{3\omega_r} & a_2 \\ a_4 & 0 & a_5 & -\omega_r \\ 0 & a_4 & \omega_r & a_5 \end{bmatrix}, B = \begin{bmatrix} \frac{1}{\sigma L_s} & 0 \\ 0 & \frac{1}{\sigma L_s} \\ 0 & 0 \\ 0 & 0 \end{bmatrix}$

$$x = \begin{bmatrix} dis_\alpha \\ dis_\beta \\ d\phi_{r\alpha} \\ d\phi_{r\beta} \end{bmatrix}, \text{ and } X = \begin{bmatrix} is_\alpha \\ is_\beta \\ \phi_{r\alpha} \\ \phi_{r\beta} \end{bmatrix}$$

The static converter is used to generate the three-phase voltage that drives the motor. We consider the converter supply as a perfect source, made up of two generators source, made of two generators of F.E.M. equal to $E/2$ connected to a point noted no. In practice, several technologies of switches are used, for example, the MOS (Metal-Oxide Semiconductor) or IGBT (Insulated Gate Bipolar Transistor) (Brown *et al.* 2011).

The role of the inverter is to supply simple AC voltages noted V_{an}, V_{bn} and V_{cn} to the motor, from a DC voltage E (supplied by a rectifier or another DC supply); the voltages supplied by the inverter form a three-phase system of variable frequency and amplitude.

The converter is controlled by the logical S_a, S_b, S_c . The combination of the different states of the

converter gives $2^3=8$ possible cases for the voltage vector V_s including two null vectors (V_0 and V_7) and six non-null vectors as shown in Figure 2.

The voltage vector is represented by the following equation 2:

$$V_s = \sqrt{\frac{2}{3}} * E(S_a + a * S_b + a^2 * S_c) \tag{2}$$

With $a = e^{\frac{j2\pi}{3}}$

The choice of the vector V_s is based on the position of stator flux (Φ_s) in the reference frame (α, β), the required variation of its modulus, its sense of rotation and the variation of the torque.

The $(\overline{\Phi_s})$ movement area is divided into six zones i , with $i = [1;6]$.

When the flux is inside a zone i one of the eight voltage vectors listed below can be used to regulate the flux and torque. (Cheok and Fukuda 2002):

If V_{i+1} is chosen then $(\overline{\Phi_s})$ increases and Γ_{em} increases.

If V_{i-1} is chosen then $(\overline{\Phi_s})$ increases and Γ_{em} decreases.

If V_{i+2} is chosen then $(\overline{\Phi_s})$ increases and Γ_{em} increases.

If V_{i-2} is chosen then $(\overline{\Phi_s})$ decreases and Γ_{em} decreases.

If V_0 and V_7 are chosen then the rotation of stator flux is stopped and a drastic decreasing of Γ_{em} is shown taking into account the value of stator remains unchanged.

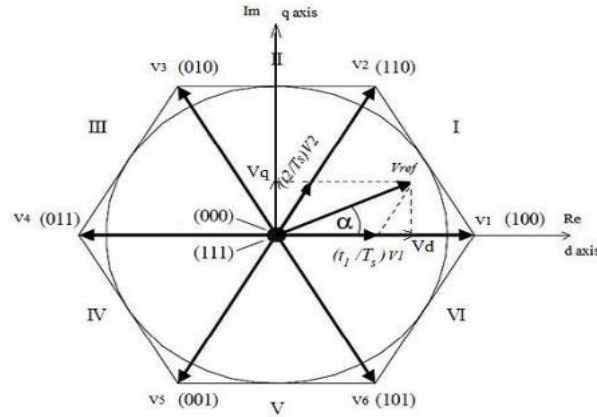


Figure 2. Voltage vector Vs based on switching states.(Ildarabadi and Ahmadi 2017)

At the beginning of the region, the vectors V_{i+1} and V_{i-2} are perpendicular to $\overrightarrow{(\Phi_s)}$, which results in a rapid evolution of the torque but a slow evolution of the flux amplitude Φ_s , whereas at the end of the region, the evolution is the opposite. With the vectors V_{i-1} and V_{i+2} , there is a slow evolution of the torque and a fast evolution of the amplitude F_s at the beginning of the zone, while at the end of the zone it is the opposite. The vectors V_i and V_{i+3} are not used whatever the direction of the torque or flux evolution because the flux component is very strong with a zero torque in the middle of the zone.

The voltage vector at the inverter's output is calculated from the torque and flux differences, as well as the position of the vector F_s , in relation to their reference (Patel *et al.* 2012). A flux estimator in modulus and position as well as a torque estimator are therefore necessary.

From the equation 3 described in the stator reference, the flux is represented as follows:

$$\Phi_s = \int_0^t (V_s - R_s * I_s) dt \quad (3)$$

The stator current is measured while the stator voltage depends on the state of the switches (S_a, S_b, S_c), and the DC link voltage E . Projecting on the two axes α and β , we will obtain the two components α and β of the estimated stator flux vector, that is:

$$\Phi_{s\alpha} = \int_0^t (V_{s\alpha} - R_s * I_{s\alpha}) dt \quad (4)$$

$$\Phi_{s\beta} = \int_0^t (V_{s\beta} - R_s * I_{s\beta}) dt \quad (5)$$

$$\hat{\Phi}_s = \hat{\Phi}_{s\alpha} + j\hat{\Phi}_{s\beta} \quad (6)$$

By applying the transformation of Concordia, we obtain:

$$V_{s\alpha} = \sqrt{\frac{2}{3}} * E * (s_a - \frac{1}{2}(s_b + s_c)) \quad (7)$$

$$V_{s\beta} = \sqrt{\frac{1}{2}} * E * (s_b - s_c) \quad (8)$$

$$V_s = V_{s\alpha} + jV_{s\beta} \quad (9)$$

Similarly, the currents $I_{s\alpha}$ and $I_{s\beta}$ are obtained from the measurement of the real currents of the machine I_{sa}, I_{sb} and I_{sc} ($I_{sa}+I_{sb}+I_{sc}= 0$) and by applying the CONCORDIA transformation, we obtain:

$$I_{s\alpha} = \sqrt{\frac{2}{3}} * I_{sa} \quad (10)$$

$$I_{s\beta} = \sqrt{\frac{1}{2}} * (I_{sb} - I_{sc}) \quad (11)$$

$$I_s = I_{s\alpha} + jI_{s\beta} \quad (12)$$

The angle and amplitude of the estimated stator flux are determined from the two flux components in frame α - β , by:

$$\Phi_s = \sqrt{\Phi_{s\alpha}^2 + \Phi_{s\beta}^2} \quad (13)$$

$$\theta_s = \text{atan}\left(\frac{\Phi_{s\alpha}}{\Phi_{s\beta}}\right) \quad (14)$$

The electromagnetic torque can be estimated from the estimated fluxes and measured currents, and can be expressed as follows equation 15:

$$Te = \frac{3}{2}p * (\Phi_{s\alpha}I_{s\beta} - \Phi_{s\beta}I_{s\alpha}) \quad (15)$$

From this equation 15, it can be seen that the accuracy of the modulus of the electromagnetic torque depends on the quality of the flux estimation and the accuracy of the stator current measurement.

This corrector is simple in its use. Its role is to maintain the end of the stator flux vector Φ_s in a circular band (Casadei *et al.* 2006). The error between

the reference flux and the estimated flux is injected into the two-level hysteresis controller, which generates at its output the Boolean variable Φ flux. (Ozturk 2008).

The main purpose of this magnetic torque corrector is to also keep the torque within the limits. The only difference with the flux corrector is that the electromagnetic torque can be positive or negative

depending on the direction of rotation of the machine (Chikhi *et al.* 2010). It is possible to propose two solutions (two-level or three-level corrector). The two-stage corrector allows controlling in one sense of rotation only, while the three-stage corrector can offer to control in case of inversion of the sense of rotation. It is strongly recommended to use in the torque, as the torque can be negative and positive at the same time.

Table 1. Vector Vs switching table

Flux	Torque	S1	S2	S3	S4	S5	S6
dΦ=1	dT=-1	V3	V4	5	V6	V1	V2
	dT=0	V0	V7	V0	V7	V0	V7
	dT=1	V5	V6	V1	V2	V3	V4
dΦ=0	dT=-1	V2	V3	V4	V5	V6	V1
	dT=0	V7	V0	V7	V0	V7	V0
	dT=1	V6	V1	V2	V3	V4	V5

The switching table is created according to the state of the Boolean variables at the output of the two flux correctors and the electromagnetic torque, as well as the area giving the information on the position of the flux vector (Casadei *et al.* 2006).

PID is widely used in industries to obtain performance on the systems to be controlled. Therefore, its main purpose is to regulate pressure, temperature, speed, flow, e.g. This controller requires a closed loop to control, providing a precise and stable response. The PID controller includes all of the necessary features, including a quick response to changes in the controller input, an increase in the control flag to reduce the error to zero, and reasonable activity inside the control blunder zone to eliminate motions. Subordinate mode improves the model system's soundness and allows for an increase in gain Kp, which increases the controller's reaction time. The mistake flag, the blunder vital, and the mistake subsidiary are the three terms that make up the PID controller's output (Abdullah and Ali 2020).

Because the integral term is present in the PI controller, the steady state error of speed is zero, making the system extremely accurate. It does not necessitate a high gain like a proportional gain controller does. However, there are certain disadvantages, such as the fact that if a very quick response is sought, the consequence paid is a greater overshoot, which is undesired. In the actual world, the PID controller seems to be a very effective approach to a variety of control problems (Aggarwal *et al.* 2015).

The mathematical form of this controller can be described as follows:

$$U(t) = Kp e(t) + Ki \int_0^t e(\tau) d\tau + Kd \frac{de(t)}{dt} \quad (16)$$

With Kp, Ki, and Kd are the parameters to be adjusted for the proportional, integral, and derivative terms, respectively, and are all non-negative (sometimes denoted P, I, and D). but in our case we just need for using PI (proportional and integral) instead of PID.

FL DTC of IM

In contrast, to a standard controller or a state feedback controller, the fuzzy logic controller (FLC) does not deal with a well-defined mathematical relationship (Saad *et al.* 2017), but instead, it uses inferences with several rules, based on linguistic variables. In this section, we will present the general procedure of designing a fuzzy logic controller.

The basic configuration of a fuzzy logic controller has three main blocks:

- Fuzzyfication.
- Inference.
- Defuzzification.

The roles of each block can be described as follows:

1) The function of the fuzzification block is to establish the value ranges for the membership functions from the values of the input variables and perform a fuzzification function that converts the

input data into suitable linguistic values (Bevrani and Daneshmand 2011).

2) The inference block is the central part of the FLC controller, which has the ability to simulate human decisions and to infer fuzzy control actions using fuzzy implication and inference rules (Mattavelli *et al.* 1997).

3) The defuzzification block also has the function of establishing the value ranges for the membership functions from the values of the output variables and performing a defuzzification that provides a non-fuzzy control signal from the derived fuzzy signal (Abdesselem, 2008). We will go even further to understand the way they operate.

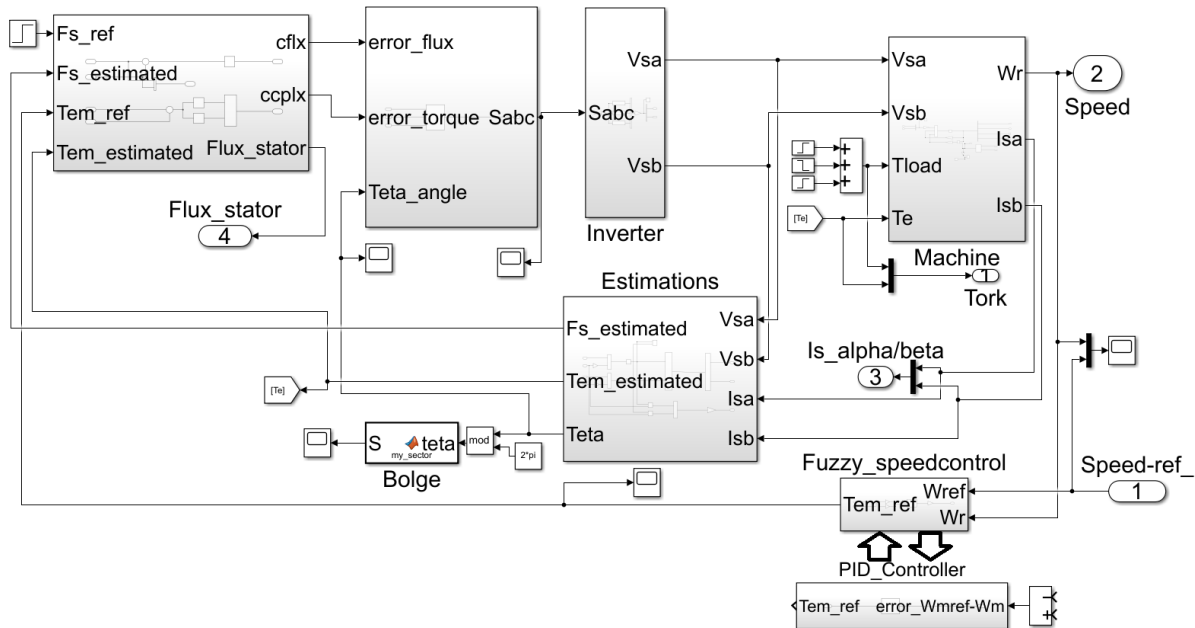


Figure 3. Matlab/Simulink block diagram of FL/PID controller

The fuzzy logic controller (FLC) is a sophisticated control technology that reflects how humans make decisions. Figure 3 shows the modelling of FL controller and PID controller in Simulink environment. Scaling factors, rule-base, and membership functions are the three basic components of the fuzzy logic speed controller (MFs). Pre-processing, processing, and post-processing are the three operational activities that make up FLC's system (Yordanova, 2015). The input variables are turned (fuzzified) into fuzzy variables through input membership functions during the pre-processing stage, which is known as fuzzification. The fuzzy rules are used for providing output fuzzy during the processing. Through output MFs, the fuzzy output variable is turned (defuzzified) towards understandable variable in the post-processing stage (Farah *et al.* 2021).

The scaling factor is a coefficient that is being employed for normalizing the fuzzy variable's value. There are three SFs in the FLC speed controller, speed error (G_e), speed error's change (G_{de}), and

output's change ($G_{\Delta T}$). The SF values typically pre-estimated depending on the motor's standard test conditions.

The variables representing the error, its change of speed and the change of output can be normalised as follows:

$$e_n = \frac{e}{G_e} \quad (17)$$

$$\Delta e_n = \frac{\Delta e}{G_{de}} \quad (18)$$

$$\Delta T_{em} = \frac{\Delta T_{em}}{G_{\Delta T}} \quad (19)$$

$G_e, G_{ce}, G_{\Delta T}$ are gains that can be a constant or a variable. The right choice of these gains allows you to guarantee stability and improve the dynamic and static performance of the desired control.

The purposed fuzzy control scheme's fuzzy control rules are designed to reduce torque ripples, and the rules can be derived from the investigators' previous experience with the DTC system (Korkmaz *et al.* 2012)

A fuzzy rule-base is a collection of IF-THEN statements that determine the fuzzy output system

Research article/Araştırma makalesi
 DOI:10.29132/ijpas.1120626

depending on the input fuzzy states (Czabanski, Jezewski and Leski, 2017). The rule base for FLC speed control having two inputs ($e_n, \Delta e_n$) and the last one is output (ΔT_{em}) described as follows:

If e_n is A and Δe_n is B then ΔT_{em} is C

The fuzzy controller is intended to improve study findings. To develop a fuzzy logic controller, some logical conditions must be understood. du is derived from the control error (e) and control error change input values (de). The error (e) is calculated using the reference and output signals. The difference

between two consecutive errors is known as the change of error. If the fuzzy logic membership is to be constructed, three or five triangles can be used. The membership of three triangles can be used to define N is negative, Z is zero, and P is positive. The membership of seven triangles can be defined as NL: negative large, NM: negative medium, NS: negative small, Z: zero, PS: positive small, PM: positive medium, PB: positive big.(Can and Sayan 2016) A rule base 7×7 will be illustrated in the table 2 shown below:

Table 2. Rule base 7×7

$e_n \backslash \Delta e_n$	NL	NM	NS	ZE	PS	PM	PL
NL	NL	NL	NL	NL	NM	NS	ZE
NM	NL	NL	NL	NM	NS	ZE	PS
NS	NL	NL	NM	NS	ZE	PS	PM
ZE	NL	NM	NS	ZE	PS	PM	PL
PS	NM	NS	ZE	PS	PM	PL	PL
PM	NS	ZE	PS	PM	PL	PL	PL
PL	ZE	PS	PM	PL	PL	PL	PL

The range of the fuzzy variable is represented graphically by membership functions (MFs). Based on the amount of MFs utilized, it breaks the range into distinct widths. There are various sorts of MFs in terms of shape, namely triangular, trapezoidal, sigmoidal, Gaussian, Z-shape, and S-shape MFs. Due to their great precision and low processing complexity, triangular and trapezoidal MFs are the most often utilized MFs in FLC speed control. Just triangular MFs will indeed be addressed in this study, and the centroid algorithm will be employed as a fuzzification tool. 3×3 , 5×5 , and 7×7 membership functions are the three most common triangle membership function sizes. The shape of these MFs will be as illustrated in Figure 4. If their breadth and

location are symmetrically designed. The breadth and membership function's position are used symmetrical, with the width between each membership function being evenly given. The membership function's existing shape is referred to as standard membership functions, but modifying the breadth and membership function's peak location effectively can improve the drive system's performance (Farah *et al.* 2021).

Parameter values of the motor used in the simulation are given in the table in Appendix.

Switching states and output voltage expressions of the inverter is shown in Table 3.

Table 3. Switching states and output voltage expressions of the inverter

Vector	s_a	s_b	s_c	v_{α}	v_{β}
v_0	0	0	0	0	0
v_1	1	0	0	$-\frac{2}{3}v_{dc}$	0
v_2	1	1	0	$\frac{1}{3}v_{dc}$	$\frac{1}{3}v_{dc}$
v_3	0	1	0	$-\frac{1}{3}v_{dc}$	$\frac{1}{\sqrt{3}}v_{dc}$
v_4	0	1	1	$-\frac{2}{3}v_{dc}$	0
v_5	0	0	1	$-\frac{1}{3}v_{dc}$	$-\frac{1}{\sqrt{3}}v_{dc}$
v_6	1	0	1	$\frac{1}{3}v_{dc}$	$-\frac{1}{\sqrt{3}}v_{dc}$
v_7	1	1	1	0	0

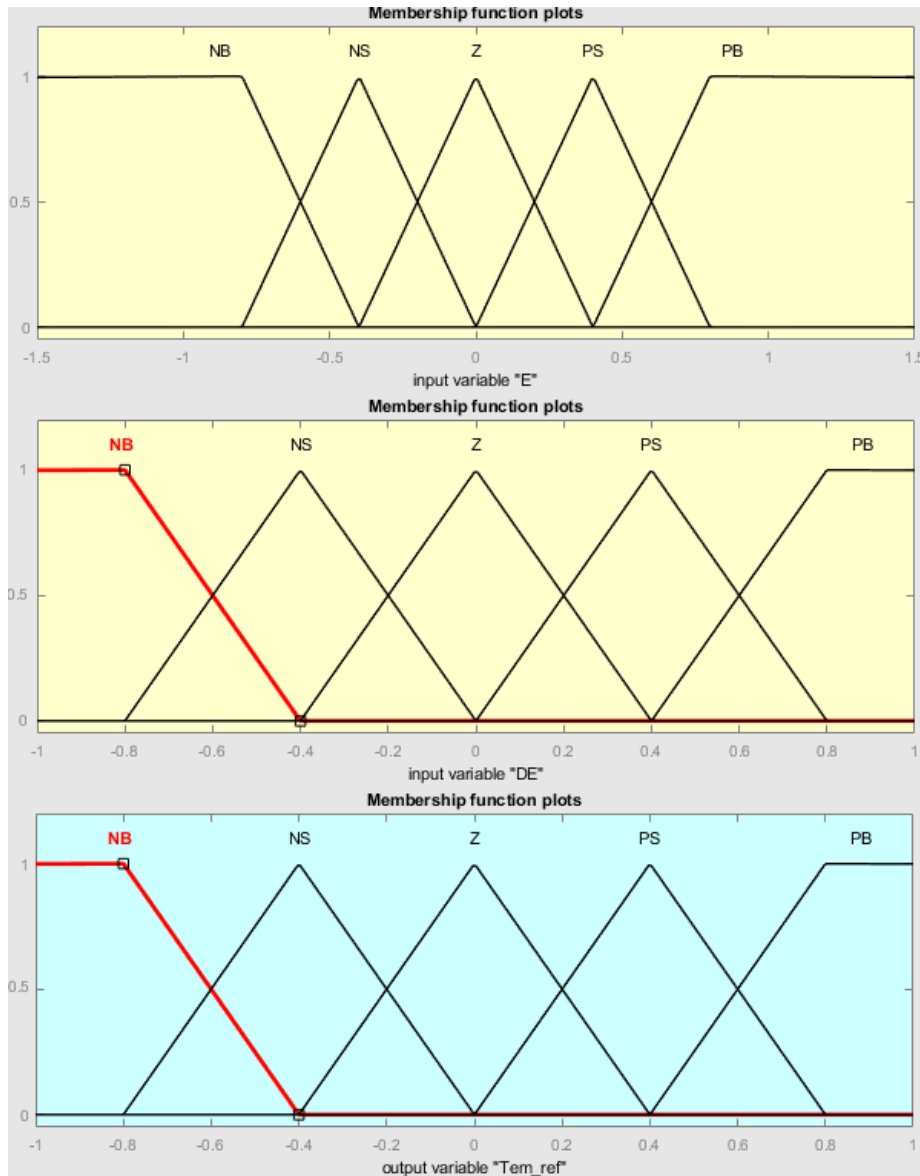


Figure 4. Triangle membership functions for all variables

RESULTS AND DISCUSSION

The direction of inversion of the motor was also carried out in order to get as much information as possible about the response to this situation. They both follow the same desired trajectory but with a slight difference in response. To begin with, we notice that at the level of the response, the PID gives a better response contrary to the fuzzy logic, which on the other hand is satisfied, with a less performing response. Indeed, when we focus on the exceeding,

the PID slightly exceeds the set point, whereas the fuzzy logic tries as fast as possible to reach the set point. As in Figure 5, Torque’s response with fuzzy logic and PID controller are shown.

As in Figure 6, when there has been a reversal of the direction of rotation at time $t=4.5$ s, the fuzzy logic gives a good impression in response unlike the PID and reaching the reference approximately.

Research article/Araştırma makalesi
DOI:10.29132/ijpas.1120626

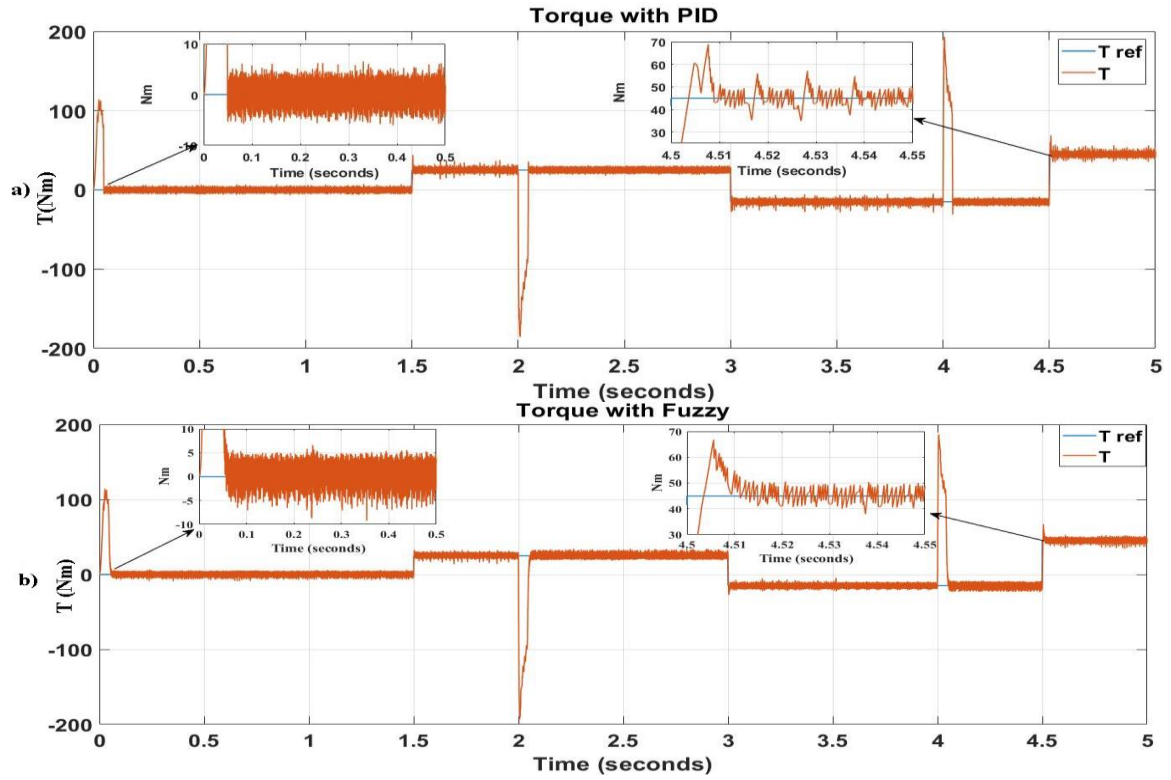


Figure 5. Torque's response with fuzzy logic (a) and PID controller (b)

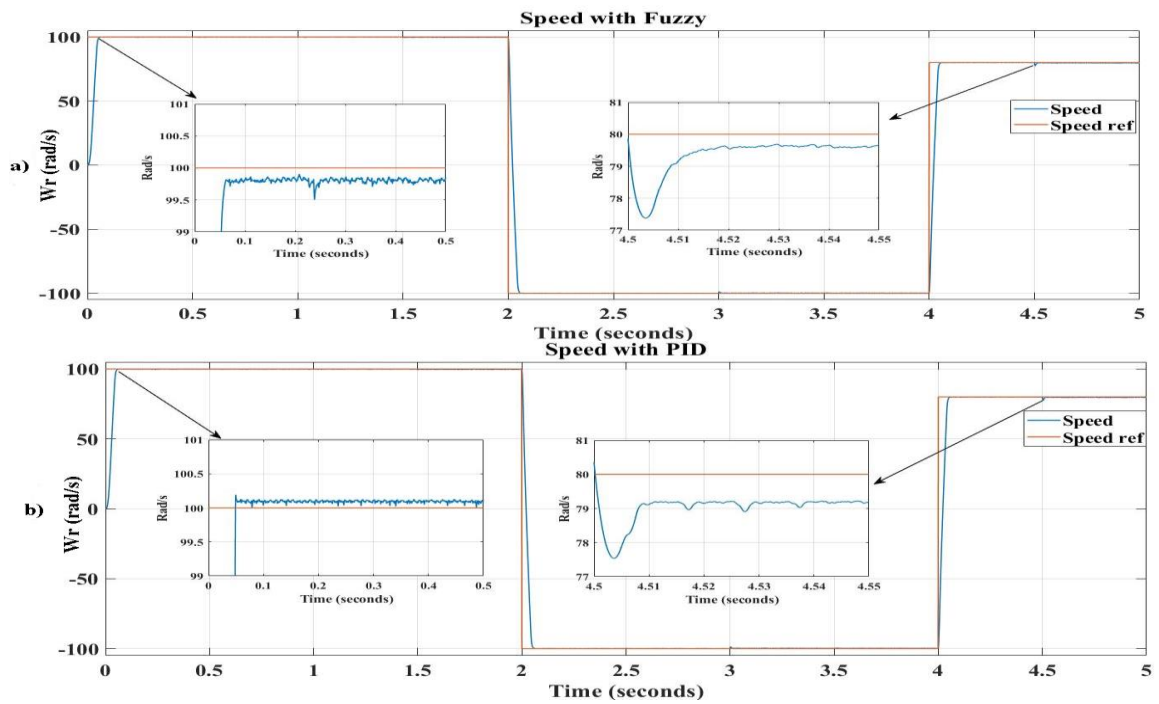


Figure 6. Speed's response with fuzzy logic (a) and PID controller (b)

Research article/Araştırma makalesi
DOI:10.29132/ijpas.1120626

CONCLUSION

The control of the main parameters of the asynchronous machine, namely the stator flux and the electromagnetic torque, is achieved by direct selection of the output voltage vectors of the inverter from a switching table. These choices are made in such a way that they can keep both quantities in a hysteresis band in the range of their reference values.

However, the existence of hysteresis controllers in the conventional direct torque control strategy generates torque and flux oscillations due to the bandwidth of the hysteresis controllers. Thus, since our study is mainly concerned with the minimization of the ripple of the electromagnetic torque and stator flux of the direct torque control applied to the three-phase induction machine.

In the previous section, the principles of fuzzy logic control and PID controller have been introduced and our choice of these methods for controlling asynchronous machines has been justified. Then, the design aspects of a fuzzy FLC controller for the speed control and PID controllers loop were presented. After selecting the Simulink simulation method and confirming its efficiency, we used this simulation under several operating conditions in order to rigorously exploit the different results that we obtained.

We can confirm according to the results that fuzzy logic offered a better result than PI controller. If we hope to get a good impression we can suggest PI-fuzzy to improve the obtained result.

CONFLICT OF INTEREST

The Authors report no conflict of interest relevant to this article.

RESEARCH AND PUBLICATION ETHICS STATEMENT

The authors declare that this study complies with research and publication ethics.

APPREHENDIX

Rs	1.2 ohm
Rr	1.8 ohm
Ls	0.1554 H
Lr	0.1584 H
Lm	0.15 H
J	0.071 kgm ²
F	0.0001 N.m.s/rad
P	2
E	240 V

Ki	2.5
Kp	52
Σ	$1 - \frac{Lm^2}{Ls * Lr}$
Ts	$\frac{Ls}{Rs}$
Tr	$\frac{Lr}{Rr}$
a ₁	$\frac{1}{\sigma Ts} + \frac{1 - \sigma}{\sigma Tr}$
a ₂	$\frac{Lm}{\sigma Lr Ls Tr}$
a ₃	$\frac{Lm}{\sigma Lr Ls}$
a ₄	$\frac{Lm}{Tr}$
a ₅	$-\frac{1}{Tr}$

REFERENCES

Abdesselem, C. (2008). Commande directe du couple du moteur asynchrone-apport de la logique floue. Thèse de maîtrise, Université de Batna, 105 pages, Algerie.

Abdullah, A. N. and Ali, M. H. (2020). Direct torque control of IM using PID controller. International Journal of Electrical and Computer Engineering, 10(1), 617.

Aggarwal, A., Rai, J. N. and Kandpal, M. (2015). Comparative Study of Speed Control of Induction Motor Using PI and Fuzzy Logic Controller. IOSR Journal of Electrical and Electronics Engineering (IOSR-JEEE), 10(2), 43-52.

Bevrani, H. and Daneshmand, P. R. (2011). Fuzzy logic-based load-frequency control concerning high penetration of wind turbines. IEEE systems journal, 6(1), 173-180.

Brown, D. W., Abbas, M. and Vachtsevanos, G. J. (2011). Turn-off time as an early indicator of insulated gate bipolar transistor latch-up. IEEE Transactions on Power Electronics, 27(2), 479-489.

Can, E. and Sayan, H. (2016). PID and fuzzy controlling three phase asynchronous machine by low level DC source three phase inverter. Tehnicki Vjesnik-Technical Gazette, 23(3).

Casadei, D., Serra, G., Tani, A. and Zarri, L. (2006). Assessment of direct torque control for induction motor drives. Bulletin of the Polish Academy of Sciences: Technical Sciences, 237-254.

Cheok, A. D. and Fukuda, Y. (2002). A new torque and flux control method for switched reluctance motor

Research article/Araştırma makalesi
DOI:10.29132/ijpas.1120626

- drives. IEEE Transactions on Power Electronics, 17(4), 543-557.
- Chikhi, A., Chikhi, K. and Belkacem, S. (2010). Induction Motor Direct Torque Control–Fuzzy Logic Contribution. IU-Journal of Electrical & Electronics Engineering, 10(2), 1207-1212.
- El-Shimy, M. E. and Zaid, S. A. (2016). Fuzzy PID controller for fast direct torque control of induction motor drives. Journal of Electrical Systems, 12(4), 687-700.
- Farah, N., Talib, H. N. and Isa, Z. (2021). Fuzzy membership functions tuning for speed controller of induction motor drive: Performance improvement. Indonesian Journal of Electrical Engineering and Computer Science, 23(3), 1258-1270.
- Ildarabadi, R. and Ahmadi, A. (2017). Simulation Study of Space Vector Pulse Width Modulation Feeding a Three Phase Induction Motor.
- Korkmaz, F., Cakir, M. F. and Topaloglu, I. (2012). Fuzzy based stator flux optimizer design for direct torque control. arXiv preprint arXiv:1212.0160.
- Korkmaz, F., Topaloğlu, İ. and Mamur, H. (2015). Fuzzy logic based direct torque control of induction motor with space vector modulation. arXiv preprint arXiv:1508.01345.
- Mattavelli, P., Rossetto, L. and Tenti, P. (1997). General-purpose fuzzy controller for DC-DC converters. IEEE transactions on Power Electronics, 12(1), 79-86.
- Mustapha E., Saad M. and Quentin C. (2022). Twelve sectors DTC strategy of IM for PV water pumping system. Materials Today: Proceedings. 51(7). 2081-2090.
- Ozturk, S. B. (2008). Direct torque control of permanent magnet synchronous motors with non-sinusoidal back-emf. Phd Thesis, Texas A&M University, 195 pages, United States.
- Patel, C., Rajeevan, P. P. and Kazmierkowski, M. P. (2011). Fast direct torque control of an open-end induction motor drive using 12-sided polygonal voltage space vectors. IEEE Transactions on Power Electronics, 27(1), 400-410.
- Saad, B. and Goléa, A. (2017). Direct field-oriented control using fuzzy logic type-2 for induction motor with broken rotor bars. Advances in Modelling & Analysis C, 72(4), 203-212.
- Said M., Aziz D., Najib E. O. and Mohammed E. M. (2022). Enhancement of the Direct Torque Control by using Artificial Neuron Network for a Doubly Fed Induction Motor. Intelligent Systems with Applications. 13, 200060.
- Soukaina E. D., Loubna L., Najib E. O. and Mustapha A. L. (2021). Sensorless fuzzy direct torque control of induction motor with sliding mode speed controller. Computers & Electrical Engineering, 96, 107490.
- Yordanova, S. (2015). Intelligent approaches to real time level control. International Journal of Intelligent Systems and Applications, 7(10), 19.